



Colour thresholds and receptor noise: behaviour and physiology compared

Misha Vorobyev^{a,*}, Robert Brandt^a, Dagmar Peitsch^a, Simon B. Laughlin^b,
Randolf Menzel^a

^a *Institut für Neurobiologie, Freie Universität Berlin, Königin-Luise-Str. 28-30, 14195 Berlin, Germany*

^b *Department of Zoology, University of Cambridge, Downing Street, Cambridge CB2 3EJ, UK*

Received 9 November 1999; received in revised form 4 April 2000

Abstract

Photoreceptor noise sets an absolute limit for the accuracy of colour discrimination. We compared colour thresholds in the honeybee (*Apis mellifera*) with this limit. Bees were trained to discriminate an achromatic stimulus from monochromatic lights of various wavelengths as a function of their intensity. Signal-to-noise ratios were measured by intracellular recordings in the three spectral types of photoreceptor cells. To model thresholds we assumed that discrimination was mediated by opponent mechanisms whose performance was limited by receptor noise. Most of the behavioural thresholds were close to those predicted from receptor signal-to-noise ratios, suggesting that colour discrimination in honeybees is affected by photoreceptor noise. Some of the thresholds were lower than this theoretical limit, which indicates summation of photoreceptor cell signals. © 2001 Elsevier Science Ltd. All rights reserved.

Keywords: Colour vision; Photoreceptor noise; Thresholds; Colour metric; Bees

1. Introduction

The best a visual system can do is to meet the limit set by noise originating in the photoreceptors. Real performance is worse than this limit, because receptor signals are corrupted by neural noise originating more proximally in the visual system. When the neural noise is high, thresholds are set by neural mechanisms, when receptor noise is dominant thresholds are set by receptors. Comparison of behavioural thresholds with the predictions based on receptor noise show that in dim light performance approaches the limit set by the receptors (Hecht, Shlaer, & Pirenne, 1942; de Vries, 1943; Rose, 1948; Reichardt, 1969; Hess, Sharpe, & Nordby, 1990; Aho, Donner, & Reuter, 1993; Warrant, Porom-bka, & Kirchner, 1996). It is, however, less easy to

decide which noise sources are dominant in the case of photopic colour thresholds.

Receptor noise can be measured directly by electrophysiological recordings. Where this is impractical, a lower limit to receptor noise can be established by estimating the quantum catch. Because the absorption of photons is a Poisson process, quantum catch fluctuates with a variance equal to mean, which generates photon noise whose relative amplitude (standard deviation/mean) is inverse proportional to the square root of light intensity (the Rose–de Vries Law). Photon noise accounts for many aspects of thresholds at low light levels (Hecht et al., 1942; Reichardt, 1969; Aho et al., 1993; Warrant et al., 1996). However, the total receptor noise is given by both photon noise and internal receptor noise. Because photon noise decreases with increasing of light intensity, one expects internal receptor noise to become increasingly prominent at high light levels. Consequently, photopic thresholds should be compared with signals and noise recorded electrophysiologically. Such photoreceptor recordings have been made in several animals (Dodge, Knight, & Toyoda, 1968; Howard, Blakeslee, & Laughlin, 1987), and photopic

* Corresponding author. Present address: Department of Biological Sciences, University of Maryland, Baltimore County, 1000 Hilltop Circle, Baltimore, MD 21250, USA. Tel.: +1-410-4553449; fax: +1-410-4553875.

E-mail address: vorobyev@umbc.edu (M. Vorobyev).

colour thresholds have been measured in many behavioural experiments (Goldsmith, 1991; Neumeyer, 1991; Menzel & Backhaus, 1991; Jacobs, 1993). However, combinations of behavioural and physiological studies of photopic colour thresholds are rare (Fain, Granda, & Maxwell, 1977). Backhaus and Menzel (1987) using an indirect estimate of receptor noise came to a conclusion that in the honeybee the role of receptor noise is negligible.

To establish the role played by different physiological mechanisms in setting behavioural thresholds, one generally requires a model of processing. Models of colour vision differ in their assumptions about the mechanisms determining colour discrimination. Early models (Helmholtz, 1896; Stiles, 1946; Trabka, 1968) did not take into account interactions between receptor mechanisms and assumed that performance is limited by receptor noise. Although these early receptor-noise-limited models explain some psychophysical data (Wyszecki & Stiles, 1982), their predictions often disagree with experimental results (Boynton, Ikeda, & Stiles, 1964). In particular, such models do not predict the shape of photopic spectral sensitivity in man (Sperling & Harwerth, 1971), fish (Neumeyer, 1984) and honeybee (von Helversen, 1972; Brandt & Vorobyev, 1997). These failures indicate that the assumptions of the early receptor-noise-limited models are not valid. Consequently, most recent models ignore receptor noise, and emphasise the importance of neural noise and opponent interactions between the receptor signals (Sperling & Harwerth, 1971; Guth, Massof, & Benzschawel, 1980; Backhaus, 1991; Yeh, Pokorny, & Smith, 1993; Cole, Hine, & McIlhagga, 1993; Sankeralli & Mullen, 1996). A common feature of these neural-noise-limited models is that they contain many parameters whose values are difficult or impossible to obtain in physiological measurements. As a result, although neural-noise-limited models explain a variety of psychophysical data, the assumptions of these models remain untested.

Recently Vorobyev and Osorio (1998) have shown that a receptor noise limited model which incorporates colour opponency predicts the shape of photopic spectral sensitivity in a number of animals, including man and honeybee (Fig. 1). An implication is that there is no obvious disagreement between the experimental results and the assumption that receptor noise is dominant. The critical parameter of this receptor-noise-limited colour opponent model is the noise level of the receptor channels. Because receptor noise can be measured in single cell recordings, behavioural thresholds can be directly compared with the model predictions.

Vorobyev and Osorio (1998) used relative rather than absolute values of receptor noise and compared the model predictions with the behavioural spectral sensitivity plotted on a relative scale. Here we relate the

absolute values of colour thresholds to the absolute values of receptor noise measured directly. We report the results obtained with the honeybee (*Apis mellifera*), a trichromatic insect, whose colour vision has been studied in detail (Menzel & Backhaus, 1991). Behavioural colour thresholds in the honeybee are easy to establish, because this insect learns colour quickly, and is highly motivated to re-visit the experimental site and to collect a reward at it. Single photoreceptor cells are accessible for intracellular recordings, and these recordings are stable for a period of time sufficient for reliable estimates of the receptor noise. The signal-to-noise ratio can be improved by spatial and/or by temporal summation of the receptor signals. We consider this possibility by taking into account the results of published behavioural studies of temporal and spatial resolution of the honeybee eye (Srinivasan & Lehrer, 1985; Giurfa, Vorobyev, Kevan, & Menzel, 1996; Giurfa, Vorobyev, Brandt, Posner, & Menzel, 1997).

2. Model

The receptor-noise-limited colour opponent model (Vorobyev & Osorio, 1998) predicts thresholds from the spectral sensitivities and noise of the photoreceptor

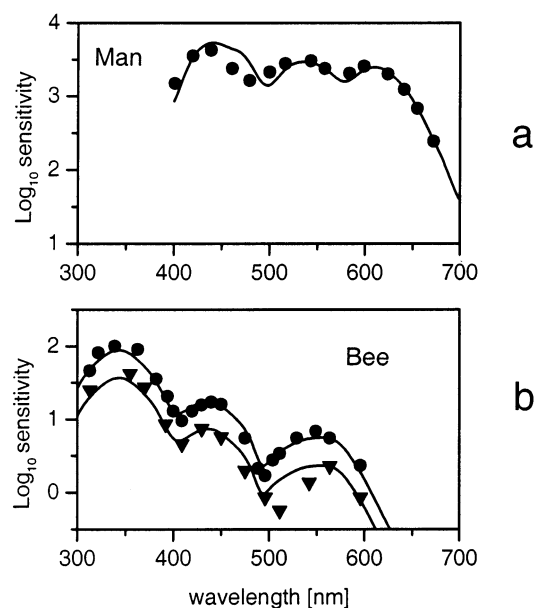


Fig. 1. Behavioural threshold spectral sensitivity (symbols) compared with predictions of the receptor-noise colour-opponent model (solid curves, Vorobyev and Osorio, 1998). Sensitivity is expressed in inverse quantum units. Curves are shifted on the sensitivity axis to match behavioural data. (a) The sensitivity of man, data of King-Smith and Carden (1976). (b) The sensitivity of two bees as recorded by von Helversen (1972). Circles denote the sensitivity of bee 25; triangles of bee 15 (the numbers of bees as in the original paper of von Helversen, 1972). The absolute sensitivity of bee 25 is 2.4 times higher than that of bee 15.

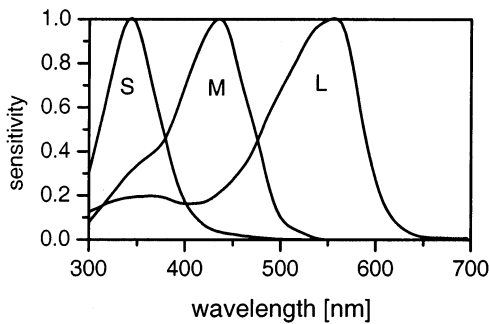


Fig. 2. The spectral sensitivities of the three receptor types of the honeybee. Sensitivity is expressed in inverse quantum units. The functions are scaled to give unity sensitivity at their peak wavelength which are 344 nm (S), 436 nm (M) and 556 nm (L) (after Menzel and Backhaus, 1991).

cells. The honeybee, *Apis mellifera*, has three types of receptors which peak in the UV (S for short-wavelength), blue (M for middle-wavelength) and green (L for long-wavelength) parts of the spectrum. We use the photoreceptor spectral sensitivity functions recorded electrophysiologically (Peitsch et al., 1992) (Fig. 2). These functions have already been used to model colour choice behaviour in the honeybee (Menzel & Backhaus, 1991; Brandt & Vorobyev, 1997; Vorobyev & Brandt, 1997; Vorobyev & Osorio, 1998).

The model (Vorobyev & Osorio, 1998) is based on three assumptions:

1. For a visual system with n receptor channels colour is coded by $n - 1$ unspecified opponent mechanisms, the achromatic signal is disregarded.
2. Opponent mechanisms give zero signal for stimuli that differ from background only in intensity.
3. Thresholds are set by receptor noise, and not by opponent mechanisms.

It is perhaps surprising that the achromatic signal is ignored, but in bright illumination for static targets subtending a large visual angle sensitivity to the achromatic component of colour is indeed low for humans (King-Smith & Carden, 1976; Thornton & Pugh, 1983), and recently it has been shown that honeybees in such conditions ignore achromatic component of colour (Backhaus, 1991; Giurfa et al., 1997; Brandt & Vorobyev, 1997; Giurfa & Vorobyev, 1998). In particular, it has been demonstrated that honeybees detect monochromatic lights on a grey background using only colour opponent mechanisms (Brandt & Vorobyev, 1997). Finally, the model accurately predicts the shape of the behavioural spectral sensitivity of the honeybee (see Fig. 1b) as reported by von Helversen (1972) (Vorobyev & Brandt, 1997; Vorobyev & Osorio, 1998).

The mathematical formulation of the model and the derivation of the formulae for di-, tri- and tetrachromatic vision are given elsewhere (Vorobyev & Osorio, 1998), but the following formulae suffice to predict

colour thresholds. Notations are listed in Table 1. Colour is defined as a point in a space whose co-ordinate axes represent the quantum catches of the receptors. Receptor quantum catches, Q_i , are given by:

$$Q_i = \int R_i(\lambda) I(\lambda) d\lambda, \quad (1)$$

where $i = S, M, L$; λ denotes wavelength, $R_i(\lambda)$ the spectral sensitivity of receptor i , $I(\lambda)$ the spectrum of light entering the eye, and integration is over the range where visual system is sensitive. It is convenient to use receptor contrast space (Cole et al., 1993), i.e. the quantum catches are normalised so that the reference stimulus yields unity quantum catch:

$$q_i = k_i Q_i, \quad (2)$$

where $k_i = 1/Q_i^r$ with Q_i^r being the quantum catch of the reference stimulus. In the case of a detection paradigm the background constitutes the reference stimulus.

To describe colour discrimination we use a classical metric approach. Discriminability of any two colours is described by the distance between them in the colour space, ΔS . Where the separation of a given pair of points in this space is below a certain threshold distance, $\Delta S'$, the colours are indistinguishable. Generally, ΔS can be arbitrarily scaled. To set the scaling factor we consider a hypothetical symmetrical colour matching experiment (MacAdam, 1942; Wyszecki & Stiles, 1982, p. 306) and assume that the accuracy of a match in this experiment is determined by sensory noise only. We define ΔS so that the unity distance corresponds to one standard deviation of the amplitude of colour mismatches. This means that if only one mechanism is present, $\Delta S = 1$ corresponds to a stimulus separation equal to one standard deviation of the noise in this mechanism.

Let f_i be the signal of receptor mechanisms i ($i = S, M, L$), Δf_i be the difference in receptor signal between two stimuli, and Δx_α be the difference in the

Table 1
Notations

λ	Wavelength
$I(\lambda)$	The spectrum of light entering the eye
$I'(\lambda)$	Threshold light intensity
$R_i(\lambda)$	Spectral sensitivity of receptor i
$r_i(\lambda)$	Receptor spectral sensitivity normalised to the reference
Q_i	Quantum catch of receptor i
q_i	Receptor quantum catch normalised to reference
f_i	Signal of receptor mechanism i
x_α	Signal of colour opponent mechanism α
e_i	Standard deviation of the noise in receptor mechanism i
ω_i	Threshold contrast of receptor mechanism i
ΔS	Distance in the colour space
$\Delta S'$	Threshold colour distance
t	Response criterion
P^F	False alarm rate

signal of colour opponent mechanism, α . Generally, Δx_α is given by a linear combination of the differences of receptor signals, i.e. $\Delta x_\alpha = \sum_{i=1}^3 F_{\alpha i} \Delta f_i$, where the coefficients $F_{\alpha i}$ describe the input of receptor i to opponent mechanism α . If only opponent signals are used for the discrimination, then the distance between the stimuli, ΔS , is given by a function of the noise and the differences in opponent signals, Δx_α ; the latter are functions of $F_{\alpha i}$ and Δf_i . Because we assume that the noise in receptor mechanisms is dominant, the discriminability of signals does not depend on how the receptor signals are combined to form opponent mechanisms. Consequently, the expression for the distance between the stimuli may not contain $F_{\alpha i}$, and the distance depends only on Δf_i and the standard deviation of the noise in receptor mechanism, e_i . Vorobyev and Osorio (1998) considered stimuli which are close to the achromatic background and have shown that if the assumptions 1–3 are correct, then in the case of trichromatic vision the colour distance is given by the following equation:

$$(\Delta S)^2 = \frac{e_S^2 (\Delta f_L - \Delta f_M)^2 + e_M^2 (\Delta f_L - \Delta f_S)^2 + e_L^2 (\Delta f_S - \Delta f_M)^2}{(e_S e_M)^2 + (e_S e_L)^2 + (e_M e_L)^2} \quad (3)$$

Receptor signals are the functions of the receptor quantum catches, and two simple models relating the receptor signals to quantum catches can be considered: (i) linear relation (Vorobyev & Osorio, 1998); (ii) log-linear relation (Vorobyev, Osorio, Bennett, Marshall, & Cuthill, 1998). Because results of our model calculations do not depend on the units in which receptor signals are measured, receptor signals can be re-scaled so that they are related to quantum catches by $f_i = q_i$ or $f_i = \ln(q_i)$ for the linear or log-linear models, respectively. Note that for the stimuli which are close to a reference both models give equal predictions, because for such stimuli

$$\Delta f_i = \Delta \ln(q_i) = \frac{\Delta q_i}{q_i} \cong \Delta q_i \quad (4)$$

Moreover, when the discrimination of stimuli from achromatic background is considered, Δf_i in Eq. (3) can be substituted by Δq_i , even if the receptor signals are related to receptor quantum catches by unknown non-linear functions (Vorobyev & Osorio, 1998).

It is important to relate the standard deviation of the noise in the receptor mechanism to the values which can be measured. In physiology it is possible to measure the signal-to-noise-ratio in a single cell. The inverse of the signal-to-noise-ratio defines the threshold contrast:

$$\omega_i = \frac{\delta q_i}{q_i} \quad (5)$$

where δq_i denotes the standard deviation of q_i . In the case of the log-linear model the standard deviation of the noise in the receptor mechanism is equal to the threshold contrast (Weber fraction), because

$$e_i = \delta f_i = \delta \ln(q_i) \cong \frac{\delta q_i}{q_i} = \omega_i \quad (6)$$

Again, in the case of stimuli which are close to the background, substitution of e_i by ω_i is valid for an unknown relation between the receptor signals and the quantum catches.

Our goal is to relate threshold light intensity, $I'(\lambda)$, to receptor noise. Let Δq_i^t be the difference in quantum catch between the stimuli at threshold. For monochromatic light of wavelength, λ , Δq_i^t is related to threshold intensity, $I'(\lambda)$, by (see Eq. (1)):

$$\Delta q_i^t = k_i R_i(\lambda) I'(\lambda) = r_i(\lambda) I'(\lambda) \quad (7)$$

where $r_i(\lambda) = k_i R_i(\lambda)$ denotes receptor spectral sensitivities normalised to the reference. Substitution of Eqs. (4), (6) and (7) into Eq. (3) gives the following expression for threshold intensity:

$$I'(\lambda) = \Delta S' \sqrt{\frac{(\omega_S \omega_M)^2 + (\omega_S \omega_L)^2 + (\omega_M \omega_L)^2}{\omega_S^2 (r_L(\lambda) - r_M(\lambda))^2 + \omega_M^2 (r_L(\lambda) - r_S(\lambda))^2 + \omega_L^2 (r_M(\lambda) - r_S(\lambda))^2}} \quad (8)$$

Eq. (8) predicts the spectral sensitivity (inverse of the threshold intensity) from the relative values of the noise in receptor channels (Vorobyev & Osorio, 1998). To estimate the absolute values of thresholds one needs to know the absolute values of threshold contrast in receptor channels, ω_i , and the value of $\Delta S'$.

Threshold colour distance, $\Delta S'$, depends on a threshold criterion, and here it corresponds to 75% of correct choices in a two-alternative forced-choice task. To calculate $\Delta S'$ we use basic concepts of signal detection theory. Our assumption is that an animal chooses a stimulus which is perceived as a more similar one to the memorised rewarded stimulus, but if the stimuli are perceived as identical they are chosen at random. The stimuli are perceived as identical if the distance between them is less than a response criterion, t . The noise limited metric is used to evaluate the distance, which means that behaviour is assumed to be matched to the noise. Because performance is corrupted by noise, identical stimuli can be perceived as different. The probability of such an event, the false alarm rate, P^F , depends on the response criterion, t . In the case of noise limited performance $\Delta S'$ also can be uniquely related to t . This allows us to establish a relation between $\Delta S'$ and P^F . Generally, the increase of the sensitivity (low $\Delta S'$) is traded against high false alarm rate, i.e. $\Delta S'$ decreases with increase of P^F (see Fig. 3). Derivation of the dependence of $\Delta S'$ on P^F is given in the Appendix A.

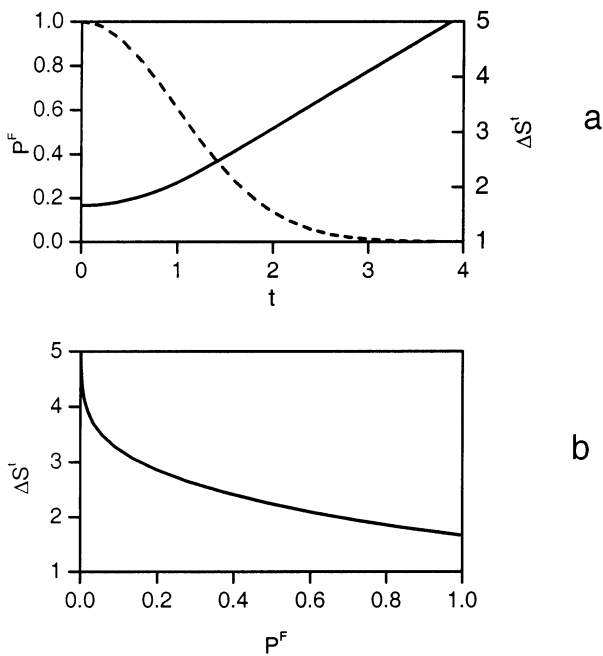


Fig. 3. The relationship of the threshold colour distance, ΔS^t , and the false alarm rate, P^F . (a) The dependence of P^F (dashed line) and ΔS^t (solid line) on the response criterion t (see Eq. (A5) and Eq. (A9)). (b) The dependence of ΔS^t on P^F as obtained from the dependence of P^F and ΔS^t on t .

3. Methods

3.1. Recordings of receptor signals and noise

The method essentially follows that of Howard et al. (1987; see also Menzel & Blakers, 1976; Peitsch et al., 1992). Honeybee workers were caught near the hive, maintained at room temperature and normal day–night cycle. The bees were restrained and their heads were immobilised with wax. A little hole was cut in the dorsal-frontal part of the cornea. KCl electrodes (100–130 M Ω) were inserted through this hole into the somata of the photoreceptors. A chloridised silver indifferent electrode was placed in the contralateral eye. Intracellular recordings of membrane potential were amplified (Axolamp 2A, Axon Instruments) and digitised at a sampling rate of 2048 Hz (CED 1401 interface). To check the quality of the recordings, the cell's membrane potential was continuously monitored (Gould A 550 chartrecorder). All experiments were done at room temperature: 20–23°C.

The eye was illuminated through a quartz light guide by a 450 W Xenon arc. The position of the light guide was adjusted to yield the maximal receptor response. Different intensities of the steady light were obtained with neutral density filters (Kodak Wratten, no. 96). Ripple in the lamp output was suppressed to less than 0.025% by using an optical feedback control system, which monitored the intensity at the entrance aperture

to the light guide. Intensity increments were generated by changing the command voltage in the feedback system. The light intensity was also measured in situ with a UV enhanced pin photodiode. Because one cannot resolve discrete quantum bumps in worker bee photoreceptors, we used fly photoreceptors to calibrate the effective intensity of our white light stimulus. Fly photoreceptors R1-6 provide an excellent biological radiometer (Howard et al., 1987). Stable intracellular recordings give consistent readings from cell to cell and they respond to a broad band of wavelengths, from the UV to the green. Because their spectral sensitivity and quantum efficiency (Dubs, Laughlin, & Srinivasan, 1981) are well established, quantum bump rates in fly can be directly converted to the intensity of natural daylight. Counts of fly quantum bumps showed that the lowest intensity of white light used in our experiments corresponds to 2.16×10^4 effective photons per receptor per second, which is 3.3 log units below full natural daylight as reported by Dixon (1978). To determine the receptor type, we recorded the responses to monochromatic lights produced with interference filters (maximum at 540, 519, 465, 428 and 353 nm). The receptor was then dark adapted for half an hour. During this adaptation the stability of the recording and sensitivity was monitored by applying 10 ms white light flashes. Signals and noise were then recorded at six different adapting intensities of white light. The intensity was increased ten-fold after each determination and the receptors were adapted for several minutes to the new background. Receptor co-ordinates of the adapting light were calculated according to Eq. (1). The highest intensity (0 log units) has the co-ordinates 17.2, 17.7 and 18.0 [$\log_{10}(\text{Photons cm}^2 \text{ s}^{-1} \text{ sr}^{-1})$] for S, M and L receptors, respectively. The voltage noise generated at each light intensity was recorded in 15 contiguous blocks of 2048 sampling points, over a period of 30 s. Responses to 100 ms increments of light intensity were recorded 100–200 times at each steady-state light condition and then averaged. The increments of the light intensity, ΔI , were proportional to the intensity of the steady state light, I , giving the increments of constant contrast $c = \Delta I/I$. The data presented here correspond to $c = 0.04$. After the experiment was finished the electrode was withdrawn from the cell and the noise of the electrode was recorded for 30 s. The photoreceptor noise amplitude and the noise power spectra were corrected by subtracting the noise of the electrode. In a separate set of experiments we measured the dynamic range of receptors by recording their responses to stimuli of different intensities.

The 15 blocks of noise recorded in each steady adaptation state were Fourier transformed; and the resulting power spectra were averaged and smoothed. The noise level was quantified by the standard deviation, σ , of the recordings. To measure the response

amplitude, ΔV , we measured the maximum of the averaged receptor response to the onset of the contrast step. The threshold contrast, ω , i.e. the contrast which yields a signal with an amplitude equal to the standard deviation of the noise, was calculated as:

$$\omega = \frac{\sigma c}{\Delta V} \quad (9)$$

The inverse of the threshold contrast is equal to the signal-to-noise ratio as defined by Howard et al. (1987).

3.2. Behavioural determination of thresholds

The procedure was similar to that used by von Helversen (1972). Freely flying individually marked honeybees were trained to collect sucrose solution from the experimental apparatus (Fig. 4). Bees were presented with two identically shaped stimuli. The stimuli were illuminated from above by broad-band light and from below by monochromatic test lights. Bees were rewarded on the unilluminated stimulus (reference only), whereas the alternative illuminated stimulus (reference + test) was not rewarded. The task of the bee was to choose the unilluminated stimulus and to avoid the illuminated one.

3.2.1. Apparatus

The test box ($80 \times 107 \times 70$ cm, $W \times H \times D$ with the front wall removed) was located in a darkened laboratory. Bees entered the box through an orifice (27×27 cm) in its back wall that was connected via a tunnel (55 cm) to an opening in the window. Artificial illumination

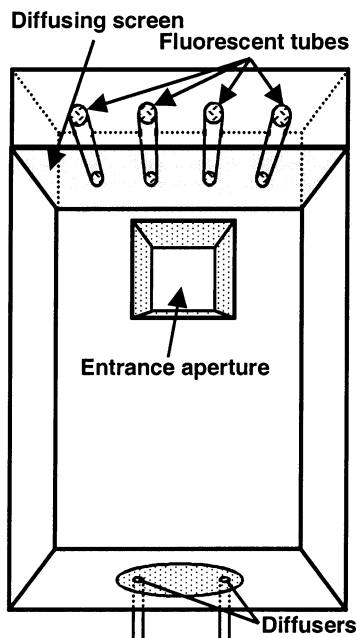


Fig. 4. The apparatus used in behavioural experiments (frontal view). Explanations in the text.

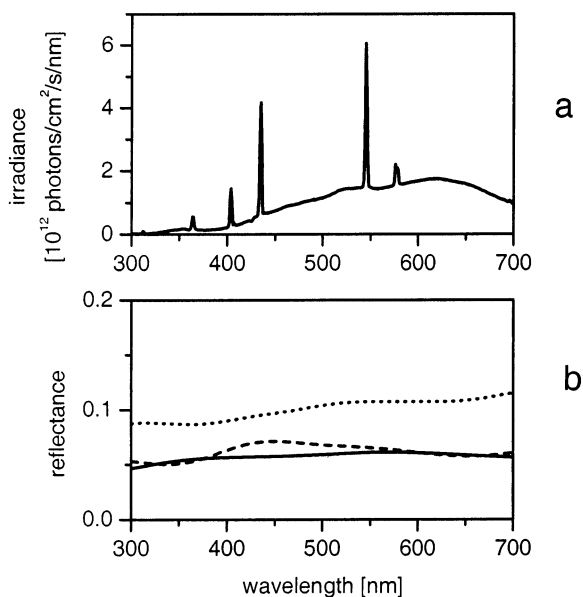


Fig. 5. The spectrum of the overhead illumination (a) and the reflectance spectra of backgrounds and diffusers used in behavioural experiments (b). The reflectance spectra of Plexiglass with HKS92 paper glued underneath is indicated by the dotted line, that of the plastic foil painted with grey paint by a dashed line, and the solid line shows the spectrum of the diffusers.

(Fig. 5a) was provided by fluorescent tubes (True Lite, Duro Test, 20) whose light had to pass a diffusing screen made of UV-transparent, sandblasted Plexiglass. To render illumination diffuse the walls were in addition covered by crumpled tin foil which also helped to minimise shadows induced by the flying bee.

The test area consisted of a circular plate (\varnothing 300 mm) in the bottom of the training box. The plate was made of UV-transparent, sandblasted Plexiglass and had two holes (\varnothing 24 mm, 180 mm apart). Each hole was covered by a slightly domed, removable circular disc made of UV-transparent, sandblasted Plexiglass. At each hole a tube (\varnothing 24 mm, 150 mm length) was fastened from below to serve as a holder for quartz light guides that were used to illuminate the discs with the stimulus light. The two discs (henceforth diffusers) constituted the stimuli. The remaining part of the test area (henceforth background) was either covered with a matt grey painted plastic foil, or a grey paper (HKS 92 N) was glued from underneath. Reflectance spectra of the two backgrounds and the diffusers are given in Fig. 5b. Note that the reflectance spectrum of diffusers is practically identical to that of one background and differs from the other one mainly in intensity.

3.2.2. Optical set-up

Monochromatic lights of 6–8 nm bandwidth were provided by a two-channel optical system consisting of a xenon arc lamp (Osram XBO 900W OFR), two

grating monochromators (Amko, Metrospec), two computer controlled circular quartz neutral density wedges and two electric shutters (Compur). Monochromatic lights were coupled into quartz light guides that led the light to the diffusers in the training box. Wavelength and radiance of the beams were calibrated using a photodiode spectrophotometer (SR01, Gröbel UV-Elektronik, Ettlingen, Germany) and a photomultiplier (International Light IL270D) at the position of the diffusers. The two beams were set to equal wavelength and radiance and the shutter of one beam was always closed. Exchanging the states of the shutters therefore, allowed us to exchange the presentation side of the stimuli.

3.2.3. Illumination

Four daylight simulating fluorescent tubes (True-Lite, Duro-Test, 20W) driven by electronic power supplies provided the illumination of the test area (rest pulsation: < 2%, peak-to-trough; frequency: 100 Hz). Illuminance of the test area was measured with a calibrated illuminance meter (UDT, model 251, S/N 44139). A dimmer was used to control illuminance measured at the bottom surface between 10 and 410 lx. A relative spectral radiant power distribution of the illuminating light was obtained using the spectrophotometer and was found to be independent of the illuminance. Experiments were performed under the illuminance of 75, 200 or 410 lx. Using the photometric measurements given in lx the relative spectra could be transformed into radiometric quantities expressed in [Photons cm⁻² s⁻¹ nm⁻¹].

The spectral radiance of the background, $I^b(\lambda)$, is then given by:

$$I^b(\lambda) = \frac{E(\lambda) B(\lambda)}{k}, \quad (10)$$

where $E(\lambda)$ is the spectral irradiance of the illumination and $B(\lambda)$ is the spectral reflectance of the background (Fig. 5a) and, k is a constant whose value depends on the geometrical properties of the illumination (Wyszecki & Stiles, 1982). If the reflecting surface were illuminated by a point source, k would be equal to π , while a value of unity corresponds to the light source subtending an angle of π sr. The light source used here

covered the entire test area and the tin foil at the walls increased the amount of the light reflected. Thus we assume $k = 1$. Substitution of Eq. (10) into Eq. (1) gives the expression for the receptor co-ordinates of the backgrounds:

$$Q_i^b = \int_{300 \text{ nm}}^{700 \text{ nm}} R_i(\lambda) E(\lambda) B(\lambda) d\lambda. \quad (11)$$

Table 2 gives receptor co-ordinates for all backgrounds and overhead illuminances used in the experiments. The spectral radiance of the diffuser, $I^d(\lambda)$, is given by

$$I^d(\lambda) = E(\lambda) D(\lambda) + I^m(\lambda), \quad (12)$$

where $D(\lambda)$ denotes the reflectance spectrum of diffuser (Fig. 5b), $I^m(\lambda)$ denotes the intensity of the monochromatic light as measured at the surface of the diffuser. Receptor co-ordinates of unilluminated diffusers (reference, Q_i^r) are given in Table 2. The monochromatic beams had a divergence angle of 12°. Consequently, Eq. (12) is valid only when the diffuser is viewed from the vertical direction (90° viewing conditions), since deviations from such viewing conditions would decrease the intensity of monochromatic light.

3.3. Training and test procedure

Honeybees raised in colonies in the garden were trained to enter the box to collect sucrose solution on the unilluminated diffuser, while the other diffuser presented a spectral light of variable intensity and was not rewarded. Only one bee was present in the apparatus during training and tests. The reward (2 M sucrose solution) was given manually as a small droplet at the tip of a Plexiglass stick. While licking, the animal was softly forced to climb the stick end, and lifted ca. 30 cm above the test area. When finished licking she flew off again and another approach flight commenced. In order to avoid learning the position of the reward the side of presentation for the unilluminated stimulus was changed in a pseudo-random manner. The diffuser which the bee landed on directly after departing from the end of the stick was recorded as a choice. If the choice was correct the bee was rewarded immediately, while after an incorrect choice she had to search again, only receiving a reward when she landed on the positive

Table 2
Receptor specific threshold contrasts for different background illuminations^a

Illuminance background	Q_s^r	Q_s^b	$\text{Log}_{10}[\omega_s]$	ω_s	Q_M^r	Q_M^b	$\text{Log}_{10}[\omega]$	ω_M	Q_L^r	Q_L^b	$\text{Log}_{10}[\omega_L]$	ω_L
410 lx HKS92	11.8	12.0	-0.67 ± 0.16	0.21	12.5	12.8	-1.13 ± 0.23	0.074	13.0	13.2	-0.93 ± 0.20	0.12
200 lx HKS92	11.5	11.7	-0.61 ± 0.15	0.25	12.2	12.5	-1.09 ± 0.23	0.081	12.7	12.9	-0.88 ± 0.20	0.13
200 lx HKS92 grey paint	11.5	11.5	-0.57 ± 0.15	0.27	12.2	12.3	-1.05 ± 0.23	0.089	12.7	12.7	-0.85 ± 0.20	0.14
75 lx HKS92	11.0	11.2	-0.52 ± 0.14	0.30	11.8	12.0	-1.01 ± 0.23	0.97	12.3	12.5	-0.81 ± 0.20	0.15

^a Receptor co-ordinates of the background Q_i^b and of a reference Q_i^r are given in $\text{log}_{10}(\text{Photons cm}^{-2} \text{ s}^{-1} \text{ sr}^{-1})$. Logarithms of threshold contrasts, ω_i (mean \pm S.D.), were obtained from the linear regression of threshold contrasts (Fig. 7c).

diffuser. Usually after 10–15 rewards the bee was satiated and returned to the hive. During that time diffusers and background were cleaned using 30% alcohol solution. For training a bright alternative was always presented. Acquisition level was reached when bees chose the unilluminated diffuser in at least 90% of the trials. Then, in a first series of tests the radiance of the alternative was reduced every two visits by 0.4 Log-units to find the approximate range where performance falls rapidly. Then stimuli within that range, one at each visit, were presented in increasing and decreasing order.

3.4. Data evaluation and statistics

The proportion of choices in favour of the unilluminated diffuser, p , was plotted versus $\log_{10}(I^m)$. In a two alternative forced choice procedure p can take values between 0.5 and 1. Threshold was defined as the response halving the admissible range, i.e. $p = 0.75$. The intensity corresponding to $p_c = 0.75$ is called the threshold radiance I' and was given by the intercept of the linear regression line drawn through the points falling in the range $0.6 < p < 0.9$ where response is approximately log-linear (von Helversen, 1972). In one experiment for each wavelength only a single choice proportion was used to determine threshold. In that case I' was obtained by extrapolation using the mean slope of the response function measured from all other bees.

The error of each threshold radiance is determined by the errors of the choice frequencies. Consider N light intensities tested. Let n_i be the number of choices and p_i be the proportion of correct choices when the animal is tested at the light intensity i , I_i . Because n_i has a binomial distribution, the standard deviation of p_i (which is denoted σ_i) is given by:

$$\sigma_i = \sqrt{p_i(1-p_i)/n_i}, \quad (13)$$

The standard deviation of the logarithm of threshold intensity, can be directly estimated from the linear regression equation. The following variables are defined:

$$x_i = \log_{10}(I_i), \quad y_i = p_i - 0.75$$

and

$$\langle x \rangle = \frac{\sum_{i=1}^N x_i}{N}, \quad \langle y \rangle = \frac{\sum_{i=1}^N y_i}{N}, \quad \langle xy \rangle = \frac{\sum_{i=1}^N x_i y_i}{N},$$

$$\langle x^2 \rangle = \frac{\sum_{i=1}^N x_i^2}{N},$$

then the linear regression equation for the threshold intensity reads:

$$\text{Log}_{10}(I') = x_0 = \frac{(\langle xy \rangle - \langle x \rangle \langle y \rangle) - (\langle y \rangle \langle x^2 \rangle)}{\langle xy \rangle - \langle x \rangle \langle y \rangle}. \quad (14)$$

The variance of $\text{Log}_{10}(I')$, $(\delta x_0)^2$ is approximately given by:

$$(\delta x_0)^2 \approx \frac{1}{N^2} \frac{(\langle x^2 \rangle - \langle x \rangle^2)^2}{(\langle xy \rangle - \langle x \rangle \langle y \rangle)^4} \sum_{i=1}^N (\langle xy \rangle - \langle y \rangle x_i)^2 \sigma_i^2. \quad (15)$$

This approximation takes into account quadratic terms of σ_i . In the case of largely overlapping σ_i , Eq. (15) overestimates the threshold variance.

4. Results

4.1. Recordings of receptor signals and noise

Flashes of bright light yield maximal receptor responses of 38 ± 8 mV, 34 ± 8 mV and 32 ± 9 mV (mean \pm S.D.) for L, M and S receptors, respectively. The dynamic range of all three receptors types covers approximately two orders of magnitude, i.e. receptors saturate for light flashes having contrast, $c \approx 100$ or less. Responses to the increments of $c = 0.04$ fall in the linear range of receptor responses at all background intensities used in the study. Examples of the responses of the three receptor types to the incremental steps ($c = 0.04$) are shown in Fig. 6. With increasing background intensity up to -1 log units, responses to superimposed intensity steps become larger, and then fall down at 0 log units (Fig. 7a). At low background intensity (but not in dark adapted cells) the recordings are noisier than at high illumination (Fig. 7b). Hence, the threshold contrast (inverse of the signal-to-noise ratio) decreases when the illumination becomes brighter (Fig. 7c). The dependence of the threshold contrast (see Eq. (6)) on the intensity of the adapting light can be approximated by a power law: $\omega = k I^a$, where a is the slope of the plots ω vs I in the double-log scale (Fig. 7c). The slope for the three receptors types are remarkably similar to each other: a obtained from the linear regression equations are equal to -0.165 ± 0.001 , -0.160 ± 0.001 and -0.180 ± 0.016 (mean \pm S.D.) for L, M and S receptors, respectively. If the fluctuations of the number of absorbed quanta determined the noise, the noise would obey the Rose-de-Vries-law (a square root dependence), and the slopes should be equal to -0.5 . If receptor noise was responsible for enforcing Weber's law, then ω would be constant ($a = 0$). The exponent of 0.16–0.18 shows that neither law can be used to predict the dependence of thresholds on light intensity. The fact that the slope is shallower than that predicted from the quantum fluctuations indicates that quantum noise alone does not determine the receptor noise. Thus, in addition to quantum noise, other processes affect the accuracy of receptor mechanisms.

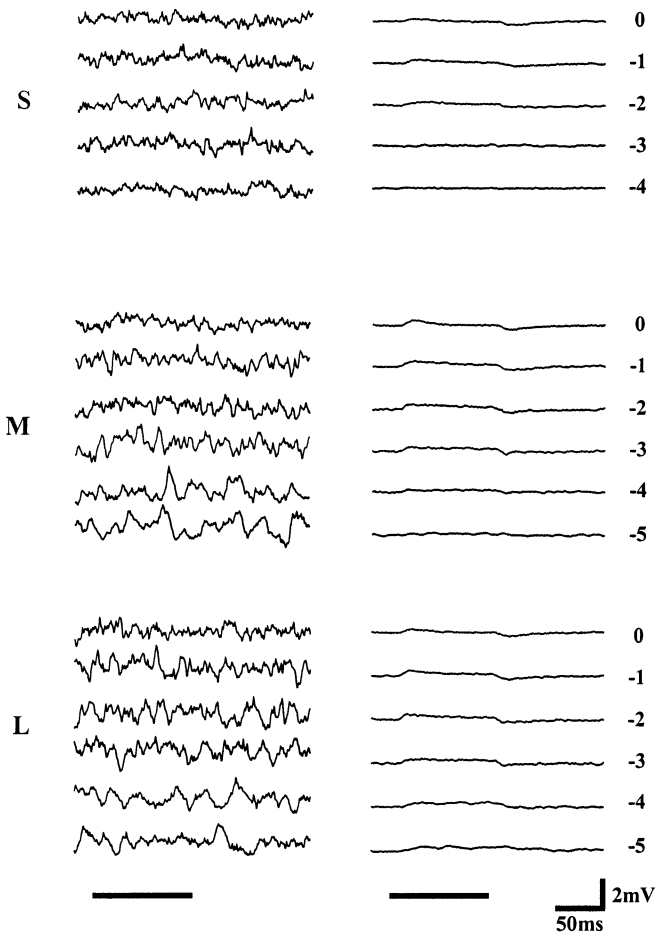


Fig. 6. Examples of responses of the three receptor types to incremental steps of the contrast, $c = 0.04$. (a) S cells; (b) M cells; (c) L cells. The left panel shows responses to single steps of light intensity which are superimposed to the different background illuminations as indicated by numbers. The highest intensity (0 log units) corresponds to receptor co-ordinates of 17.2, 17.7 and 18.0 [$\log_{10}(\text{Photons cm}^2 \text{ s}^{-1} \text{ sr}^{-1})$] for S, M and L receptors, respectively (Section 3). The right panel shows the curves averaged from 100 to 200 responses. The horizontal bar indicates the time of light stimulation.

Temporal resolution of the photoreceptors is limited by the duration of a single quantum event. In honeybees single quantum events cannot be recorded. However, the limit of temporal resolution can be estimated from the temporal properties of the receptor noise (Dodge et al., 1968). A rough estimate of the event duration, τ , is given by fitting the power spectra, $P(f)$, by a Lorentzian:

$$P(f) = \frac{A}{1 + (2\pi f\tau)^2} \quad (16)$$

where f denotes the frequency and A is a constant (Howard et al., 1987). The power spectra are shown in Fig. 8, and the event duration obtained from the noise spectra are listed in Table 3. Although the data scatter considerably, it is evident that with increasing light intensity the event duration becomes shorter. The event

duration varies from approximately 10 ms for dark adapted cells to 3 ms at higher intensities. These values agree well with the estimates of the temporal resolution obtained in behavioural experiments: Srinivasan and Lehrer (1985) have shown that flicker fusion frequency is close to 200 Hz which corresponds to an event duration of 5 ms. This similarity indicates that photoreceptors limit the temporal resolution of the bee eye.

4.2. Increment thresholds as a function of wavelength and mean luminance

Each bee ($N = 7$) was tested at a number of different wavelengths in the range 350–550 nm. Most thresholds were derived from two to four relative choice frequencies. An exception from this rule was a bee tested at 200 lx on a grey paint-HKS92 background, where each threshold was determined from a single choice proportion (Section 3). In this case we recorded thresholds with the same bee at 15 different wavelengths.

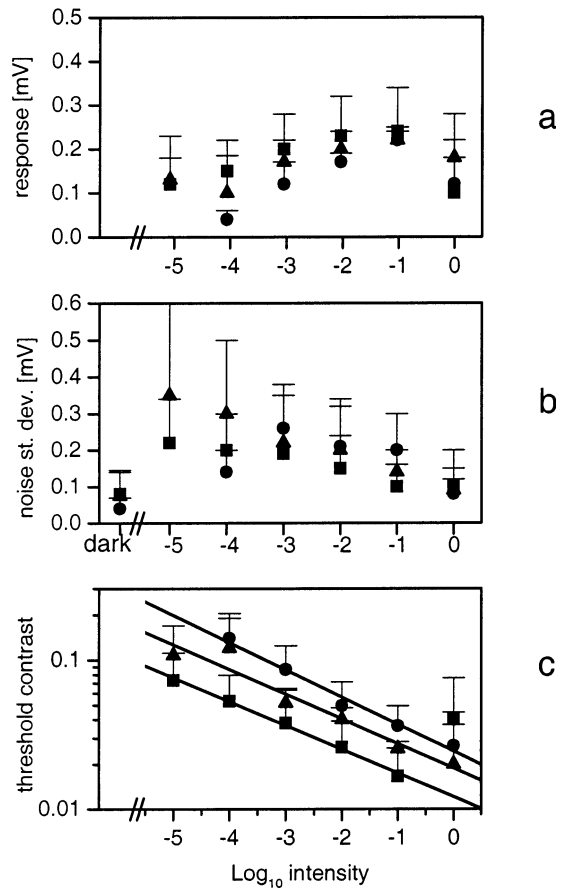


Fig. 7. The dependence of the receptor response (a), receptor noise (b) and threshold contrast (c) on the intensity of the adapting light. Error bars show the standard deviation. Circles, triangles and squares correspond to S, M and L cells, respectively. The straight lines show linear regression. In the case of L cells (squares) the threshold contrast corresponding to zero log units is an out-liar and it was disregarded in the linear regression. For each receptor type the light intensity expressed in relative units was converted into the quantum catch (see Section 3).

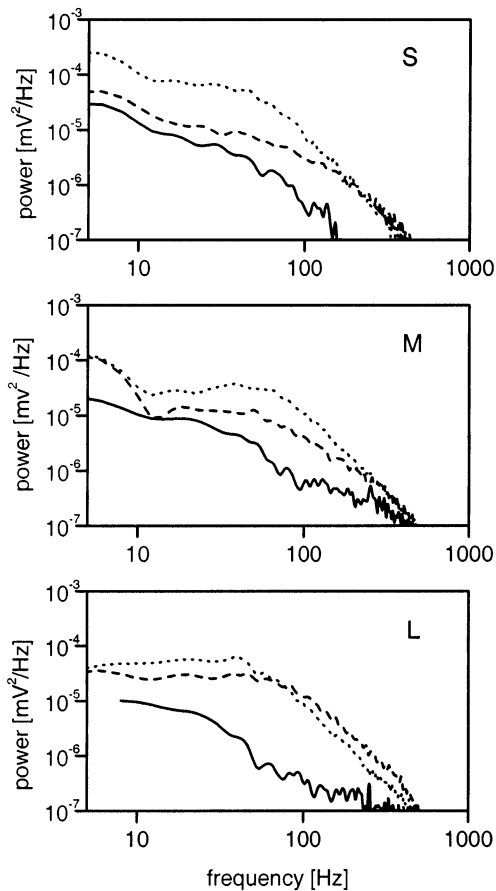


Fig. 8. Examples of the noise power spectra recorded in single cells. The panels correspond S, M, and L cells. Solid line corresponds to dark adapted cells; dashed and dotted lines correspond respectively to -3 and -1 log units.

The threshold is uniquely defined only if the proportion of correct choices increases monotonically with increasing radiance of the stimulus. Usually response functions are monotonic. However, for some bees tested on different days the position of the curve along the abscissa was shifted (Fig. 9). In this case the variability of thresholds significantly exceeds the error bars. Hence, this variability cannot be explained by the lim-

Table 3
The event duration depending on the intensity of the adapting light^a

Illuminance (relative \log_{10} units)	τ_S	τ_M	τ_L
Dark	8.8 ± 12.0	9.7 ± 4.8	12.1 ± 3.4
-5	–	7.7 ± 5.3	8.8 ± 2.9
-4	5.9 ± 2.4	3.6 ± 1.1	5.3 ± 0.7
-3	8.1 ± 6.2	3.2 ± 0.9	3.9 ± 1.6
-2	13.4 ± 14.4	5.8 ± 4.2	3.5 ± 1.0
-1	2.6	8.5 ± 4.9	4.0 ± 2.2
0	–	8.7 ± 5.6	4.0 ± 1.9

^a Event duration, τ_p , was estimated using Eq. (16) from the power spectra (Fig. 8); $\tau_p \pm$ S.D., is given in ms.

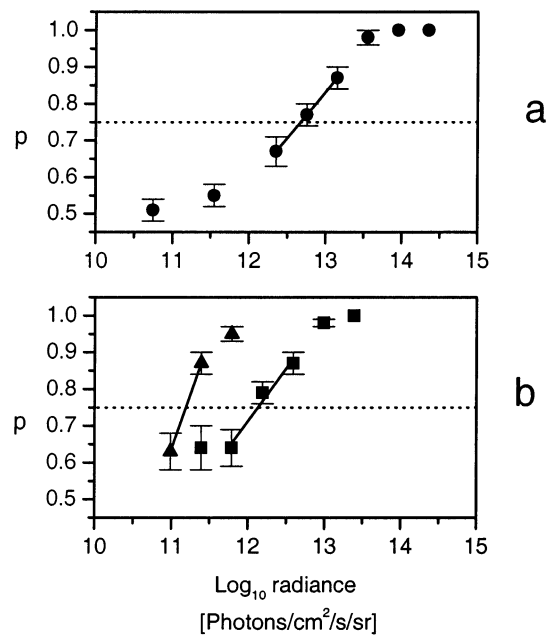


Fig. 9. Examples of the choice behaviour of individual bees depending on the intensity of the monochromatic light. The proportion of correct choices, p , is plotted along the ordinate axis. The error bars show the standard error of the proportion of correct choices (Eq. (13)). The solid line shows linear regression over the points having p in the range of 0.6–0.9. An intercept of the linear regression line with the line corresponding to $p = 0.75$ defines the threshold intensity. (a) A bee tested with 490 nm light at the illuminance 75 lx and the Plexiglass/HKS92 background. (b) A bee tested with 438 nm light at the illuminance 410 lx and the Plexiglass/HKS92 background. Note that this bee shows two different thresholds. In this case the experiments were performed with a 3-day interval.

ited number of choices. Also, the variability of thresholds obtained with different bees significantly exceeds the error of threshold estimates for individual bees (Fig. 10).

4.3. Comparison with thresholds estimated from the receptor noise

A theoretical estimate of thresholds was made with Eq. (8), which relates the threshold intensity of the monochromatic light, I' , to the threshold contrast of the receptor mechanism, ω_p . The threshold contrast recorded in a single photoreceptor cell depends on background light intensity (Fig. 7). To relate physiological measurements to behavioural data we calculated the receptor quantum catches (see Eq. (11)) for the eye viewing backgrounds illuminated by lights of different intensities (Table 2), and estimated threshold contrasts corresponding to these quantum catches using linear regression (see Fig. 7c). Results of the calculations are shown in Table 2. The threshold contrasts so obtained refer to the level of noise in single receptor cells. However, visual systems may improve signal-to-noise ratio by temporal and/or by spatial summation. Be-

cause the temporal resolution of the bee eye (Srinivasan & Lehrer, 1985) is close to the limit set by temporal resolution of the single photoreceptor cells, we assume that threshold contrast is not altered by temporal integration of receptor signals. We consider spatial summation and regard three cases:

1. No summation, i.e. it is assumed that the animal relies on the output of a single receptor triplet (one receptor cell for each spectral receptor type). This case will be referred to as the ‘receptor triplet’ assumption. This assumption sets an upper bound for the influence of photoreceptor noise.
2. Summation within one ommatidium. Each ommatidium receives information from a distinct point in space, so that it can be considered as the smallest spatial sampling unit. Summation within one om-

matidium would improve signal-to-noise ratio without sacrificing spatial resolution. This will be referred to as the ‘one ommatidium’ assumption. The effective noise in each colour channel will be reduced by a square root of the number of cells. Assuming that the number of receptor cells, N_{is} , is 3, 2 and 4 for S, M and L receptors, respectively (Menzel & Blakers, 1976) we come to the conclusion that the noise in S, M and L receptors should be divided by 1.73, 1.41 and 2, respectively.

3. Summation across the ommatidia forming a chromatic receptive field. This assumption will be referred to as the ‘chromatic receptive field’ assumption. This case accounts for the fact that the minimum visual angle by which a colour stimulus can be detected on the basis of its chromatic properties is 15° (Giurfa et al., 1996). In the frontal eye region that is used for colour discrimination, a 15° stimulus covers 59 ommatidia (Giurfa et al., 1996). Thus the effective noise would in addition be reduced by the square root of 59, i.e. by 7.7. Note that this reduction represents an absolute lower limit of thresholds, because it is assumed that the signals of all ommatidia are summed linearly with equal weights and that the process of summation does not introduce additional noise. Moreover, it is not known whether all the receptor cells within the ommatidia contribute to the chromatic visual subsystem. For example, the 9th UV sensitive cell is small, and it has been proposed that it is not used for colour vision (Menzel & Snyder, 1975)

Most of the measured thresholds are close to the predictions of the single triplet and single ommatidium

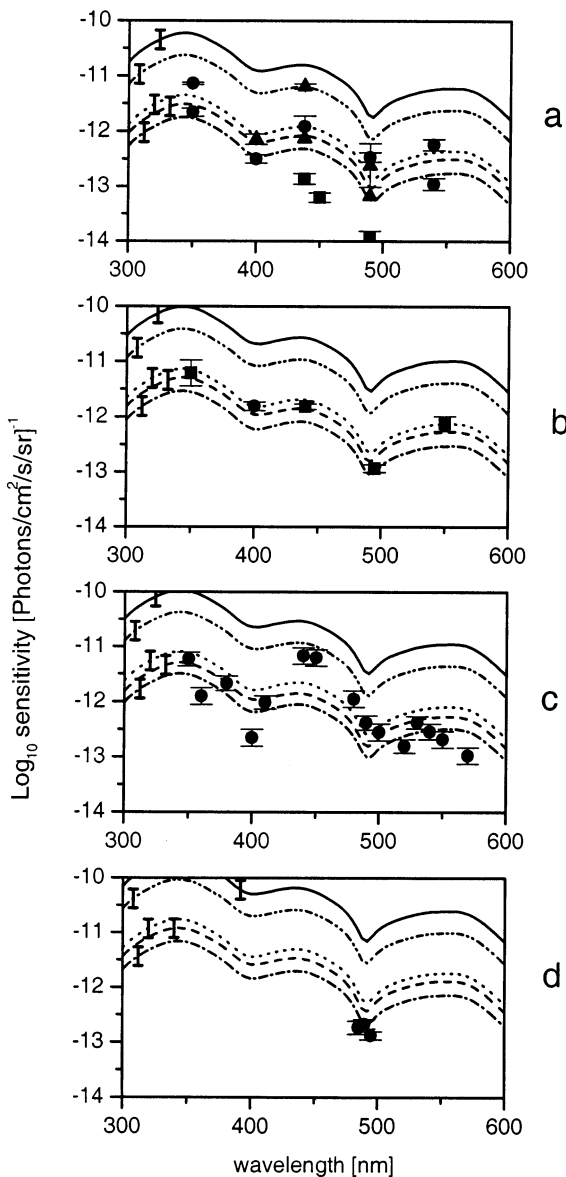


Fig. 10.

Fig. 10. Behavioural sensitivity (inverse of threshold intensity) to the monochromatic light depending on its wavelength. The panels differ with respect to the illumination/background condition. (a) 410 lx, Plexiglass/HKS92. (b) 200 lx, grey paint. (c) 200 lx, Plexiglass/HKS92. (d) 75 lx, Plexiglass/HKS92. Different symbols within each panel correspond to different bees. Error bars indicate standard errors (Eq. (9)). The data presented in the panel c were obtained by extrapolation from a single choice proportion for each wavelength (see Section 3). The lines indicate the predictions (Eq. (8)) based on the receptor specific threshold contrast (Table 2). The estimates of threshold contrast are based on the mean of physiological measurements. The model predictions may vary due to the scatter of physiological measurements (Fig. 7); the thick error bars on the curves correspond to the standard deviation of the model prediction. The curves differ with respect to the degree of spatial summation and threshold distance, $\Delta S'$, which, in turn, depends on false alarm rate, P^F (Fig. 3). Calculations are either for $P^F = 1$ (the upper limit of sensitivity) or for $P^F = 0.01$. Dotted curve: discrimination is based on the output of a single receptor triplet, $P^F = 1$. Dashed-single-dotted curve: discrimination is based on the output of a single receptor triplet, $P^F = 0.01$. Dashed curve: summation of the receptor signals within one ommatidium, $P^F = 0.01$. Solid curve: summation over the chromatic receptive field consisting of 59 ommatidia, $P^F = 1$. Dashed-double-dotted curve: summation over the chromatic receptive field consisting of 59 ommatidia, $P^F = 0.01$.

hypothesis (Fig. 10) and none of them are lower than the predictions of the chromatic summation assumption. Interestingly, there is also one threshold located close to the theoretical limit set by the chromatic summation assumption. Bees on the grey background (Fig. 10b) behave nearly perfectly consistent with the receptor triplet model predictions.

5. Discussion

Given the scatter of the behavioural data, the thresholds predicted from electrophysiological measurements of receptor noise agree reasonably well with the measured values. This agreement holds over a range of background illumination conditions and test wavelengths, suggesting that receptor noise, indeed, plays an important role in setting the thresholds. The simulation developed by Backhaus and Menzel (1987) led them to the opposite conclusion. This contradiction is explained by differences between the methods of calculating receptor noise. Backhaus and Menzel (1987) took preliminary recordings of voltage noise and converted these to noise-to-signal ratios by dividing through by the maximum amplitude of the photoreceptor response. Because the maximum amplitude is evoked by saturating stimuli, their noise to signal ratio, 0.3%, is unrealistically low and it reduces the effects of photoreceptor noise to insignificant levels. The method we adopt, relating noise to responses to stimuli of low contrast, is appropriate for increment thresholds, and is more realistic for most applications. Our method demonstrates very significant levels of receptor noise under the conditions of the behavioural tests, with noise-to-signal ratios that are two orders of magnitude higher than Backhaus and Menzel's. We can easily dismiss the possibility that our high noise values are an artefact, generated by poor recordings and inadequate stimuli. Menzel and Backhaus's noise-to-signal ratio of 0.3% is an order of magnitude below the lowest ratios measured in blowfly photoreceptors in bright light (Howard et al., 1987). With their larger rhabdomeres and a broader spectral sensitivity, blowfly photoreceptors should perform slightly better than bee cells. Our measurements are in line with this prediction. The best noise-to-signals ratios that we have measured in bee approach, but do not reach, the lowest values found in fly (Howard et al.). We are confident, therefore, that receptor noise is of sufficient magnitude to determine thresholds.

Backhaus and Menzel tested their simulation against von Helversen's (von Helversen, 1972) classic wavelength discrimination function. Wavelength discrimination could be close to the limit set by receptor noise. However, we cannot use our data to compare wavelength discriminations directly with thresholds set by

noise, because the task of discriminating of two suprathreshold spectrally pure lights (wavelength discrimination) is different from the discrimination threshold spectral stimuli from an achromatic background (spectral sensitivity). There are two main reasons why wavelength discrimination is difficult to analyse: (i) the receptor signal-to-noise ratios, as they are usually measured, correspond to the task of detection of stimuli on an adapting background, rather than to discrimination of two stimuli which differ from background substantially; (ii) simple models are, generally, not suited for the analysis of discrimination of highly saturated stimuli (Brandt & Vorobyev, 1997; Vorobyev & Osorio, 1998).

Calculations based on the ratio of receptor noise values (Vorobyev & Brandt, 1997; Vorobyev & Osorio, 1998) have previously explained the shape of the spectral sensitivity curve of the honeybee as reported by von Helversen (1972) (Fig. 1). However, in the present study the thresholds for most of the bees do not lie on the theoretical curves, which can be attributed to the scatter. Variability in absolute sensitivity between individual bees has been already reported; for example, the absolute sensitivity of bee 25 in von Helversen's study (von Helversen) is 2.4 times higher than that of the bee 15. Also, changes of thresholds within the same individual bee have been described by von Helversen, 1972. Here we show that the variability of thresholds is not attributable to statistical error in estimating the thresholds from the limited number of choices, but rather to changes in the behaviour of bees. Since we worked with freely flying bees the precise position where they made a decision for a particular stimulus is unknown. This can partly explain the variability of thresholds: the intensity of monochromatic light decreases rapidly when the viewing angle to the illuminated stimulus deviated from 90° (Section 3).

Apart from such deviations from the optimal 90° viewing conditions the occurrence of thresholds higher than the model predictions can be explained by noise added in further stages of neural processing. An alternative explanation refers to the decision rule adopted by bees (see Section 2). The threshold colour distance corresponding to 75% correct choices depends on the false alarm rate, P^F (Fig. 3). In the limiting case of P^F being equal to unity threshold reaches its lowest limit. In reality thresholds are higher (Fig. 10, dashed-dotted curves), and the actual value of threshold is determined by a trade-off between the low false alarm rate and high sensitivity of vision.

The occurrence of thresholds lower than those predicted by the single ommatidium hypothesis indicates that signal-to-noise ratio is improved by spatial or temporal summation. Because the temporal resolution

of the honeybee eye as derived from the flicker fusion experiments (Srinivasan & Lehrer, 1985) agreed well with the estimate of the temporal resolution of the single photoreceptor cell, it is unlikely that temporal summation could significantly decrease the noise in receptor channel. On the other hand, the hypothesis that the signal-to-noise ratio is improved by spatial summation of receptor signals agrees with the fact that spatial resolution of chromatic vision in the bee is significantly worse than that predicted from the optics of the bee eye (Giurfa et al., 1996). The accuracy of our data does not allow an estimate of the number of ommatidia involved in summation. But since none of the thresholds is lower than the predictions of the chromatic receptive field hypothesis, our results do not contradict the estimates of the receptive field size as derived from the study of the angular resolution of honeybee colour vision (Giurfa et al., 1996).

Our conclusion that signal-to-noise ratio is improved by summation of the signals of several photoreceptor cells is consistent with physiological studies of the fly eye (Howard et al., 1987) and with behavioural measurements of visual acuity in walking honeybees tested in conditions of dim illumination (Warrant et al., 1996). In conditions of dim light bees also sacrifice temporal resolution in order to improve the signal-to-noise ratio (Warrant et al., 1996). This can be explained by the fact that receptor cells become slower when the light intensity decreases (see Table 3).

Finally, the results presented here give strong evidence in favour of the hypothesis that receptor noise affects the accuracy of colour discrimination. However, because the number of receptor cells involved in summation is not known, we cannot conclude that thresholds are set only by receptor noise with neural noise being negligible. We think that both receptor noise and more proximal neural noise affect thresholds. If the noise generated in one of the mechanisms, for example in receptors, was negligible, selection pressure would not maintain the low level of noise in this mechanism. Consequently, during evolution the noise in either mechanism would have been allowed to increase until its influence on the behaviour would have become notable.

Acknowledgements

We would like to thank Daniel Osorio for fruitful discussions and helpful comments on the manuscript, and two referees for helpful comments and corrections of the manuscript. The work was supported by Alexander-von-Humboldt-Foundation, Nafög foundation and DFG.

Appendix A

Consider two stimuli: one identical to a rewarded stimulus, A, and the other one, B, whose colour distance to a rewarded stimulus (the stimulus A) is equal to a . The colour distance is calculated according to the noise defined metric (see Eq. (3)). Perception is inevitably corrupted by noise, and the actual perceived distances to the rewarded stimulus are described by random variables which we denote as $\Delta\xi_A$ and $\Delta\xi_B$ for the stimuli A and B, respectively. The probability, p^{cor} , that the correct stimulus, A, is chosen, and the probability of false alarm, P^F , can both be calculated from the probability density distributions of $\Delta\xi_A$ and $\Delta\xi_B$. The latter, in turn, can be obtained from the distribution of receptor noise. We assume that stimuli are perceived as different if the distance between them exceeds a given response criterion, t , and derive the formulae which relate P^F to t , and P^{cor} to the distance between the stimuli, a , and to the response criterion, t . If the receptor noise has a Gaussian distribution, then the distribution of signals corresponding to stimuli A and B in the colour opponency plane has a two-dimensional Gaussian distribution with a centre at the points A and B, respectively. The assumption that the noise has a Gaussian distribution is not crucial, and similar calculations can be performed for other noise distributions, for example, for a Poisson distribution. Note that the Poisson distribution, which is valid when the noise is defined by fluctuations of absorbed quanta only, converges to a Gaussian distribution as the average number of absorbed quanta increases. We use a polar co-ordinate system (r, Ψ) with an origin at the point A. In the case of stimulus A, the Gaussian distribution of the signals is given by:

$$g_A(r, \psi) dr = \frac{1}{2\pi} \exp\left(-\frac{r^2}{2}\right) r d\psi dr. \quad (\text{A1})$$

Similarly, for stimulus B, separated from A by a distance a , the Gaussian distribution of the signals is given by:

$$g_B(r, \psi) d\psi dr = \frac{1}{2\pi} \exp\left(-\frac{r^2 - 2ra \cos(\psi) + a^2}{2}\right) r d\psi dr. \quad (\text{A2})$$

The standard deviation in Eq. (A1) and Eq. (A2) is simply equal to unity, because we assume that unity distance in colour space corresponds to one standard deviation of the noise. The distributions of the distances $\Delta\xi_A$ and $\Delta\xi_B$ — $f_A(r) dr$ and $f_B(r) dr$ — are obtained by averaging Eq. (A1) and Eq. (A2) over the angle Ψ :

$$f_A(r) dr = \left(\int_0^{2\pi} \frac{1}{2\pi} \exp\left(-\frac{r^2}{2}\right) r d\psi \right) dr = \exp\left(-\frac{r^2}{2}\right) r dr \quad (\text{A3})$$

$$\begin{aligned}
 & f_B(r)dr \\
 &= \left(\int_0^{2\pi} \frac{1}{2\pi} \exp\left(-\frac{r^2 - 2ra \cos(\psi) + a^2}{2}\right) r d\psi \right) dr \\
 & \quad \quad \quad (A4) \\
 &= \exp\left(-\frac{a^2}{2}\right) \exp\left(-\frac{r^2}{2}\right) I_0(ra) r dr,
 \end{aligned}$$

where I_0 denotes the modified zero order Bessel function of the first kind.

For a given response criterion, t , the probability of false alarm is equal to the probability that $\Delta\xi_A$ is greater than t , i.e. $P^F = P(\Delta\xi_A > t)$. From Eq. (A3) it follows that

$$P^F = P(\Delta\xi_A > t) = \int_t^\infty f_A(r) dr = \exp\left(-\frac{t^2}{2}\right). \quad (A5)$$

This equation relates the response criterion to the false alarm rate. To evaluate P^{cor} we consider the probability that A is perceived as more similar to the rewarded stimulus than B, $P(\Delta\xi_A < \Delta\xi_B - t)$, and the probability that it is not certain which stimulus is more similar to the rewarded one, $P(|\Delta\xi_A - \Delta\xi_B| < t)$. We assume that if it is not clear which stimulus is more similar to a rewarded one, then the stimuli are chosen at random. Consequently, the probability that the correct stimulus A is chosen is given by:

$$P^{\text{cor}} = P(\Delta\xi_A < \Delta\xi_B - t) + 0.5P(|\Delta\xi_A - \Delta\xi_B| < t). \quad (A6)$$

From Eq. (A4) and Eq. (A3) it follows that:

$$\begin{aligned}
 P(\Delta\xi_A < \xi_B - t) &= \int_t^\infty f_B(y) \int_0^{y+t} f_A(r) dy dr \\
 &= \exp\left(-\frac{a^2}{2}\right) \int_t^\infty \exp\left(-\frac{y^2}{2}\right) I_0(ya) \\
 &\quad \times \left(1 - \exp\left(-\frac{(t-y)^2}{2}\right)\right) y dy
 \end{aligned} \quad (A7)$$

and

$$\begin{aligned}
 P(|\Delta\xi_A - \Delta\xi_B| < t) &= \int_0^t f_B(y) \int_0^{y+t} f_A(r) dx dy \\
 &\quad + \int_t^\infty f_B(x) \int_{y-t}^{y+t} f_A(x) dx dy \\
 &= \exp\left(-\frac{a^2}{2}\right) \int_0^t \exp\left(-\frac{y^2}{2}\right) I_0(ya) \\
 &\quad \times \left(1 - \exp\left(-\frac{(y+t)^2}{2}\right)\right) y dy \\
 &\quad + \int_t^\infty \exp\left(-\frac{y^2}{2}\right) I_0(ya) \\
 &\quad \times \left(\exp\left(-\frac{(y-\frac{t}{2})^2}{2}\right) - \exp\left(-\frac{(y+t)^2}{2}\right)\right) y dy.
 \end{aligned} \quad (A8)$$

Substitution of Eq. (A7) and Eq. (A8) into Eq. (A6) gives the expression for P^{cor} as a function of a distance a and response criterion, t . The threshold colour distance $\Delta S'$ is equal to a distance a yielding 75% correct choices. Consequently, the threshold colour distance is obtained from the following equation:

$$P^{\text{cor}}(\Delta S', t) = 0.75, \quad (A9)$$

where $\Delta S'$ substitutes for a . Solution of this equation for each value off gives the dependence of $\Delta S'$ on t ; the latter, in turn, is related to P^F by Eq. (A5).

References

- Aho, A. C., Donner, K., & Reuter, T. (1993). Retinal origins of the temperature effect on absolute visual sensitivity in frogs. *Journal of Physiology (London)*, 463, 501–521.
- Backhaus, W. (1991). Color opponent coding in the visual system of the honeybee. *Vision Research*, 31, 1381–1397.
- Backhaus, W., & Menzel, R. (1987). Color distance derived from a receptor model of color vision in the honeybee. *Biological Cybernetics*, 55, 321–331.
- Boynton, R. M., Ikeda, M., & Stiles, W. S. (1964). Interactions among chromatic mechanisms as inferred from positive and negative increment thresholds. *Vision Research*, 4, 87–117.
- Brandt, R., & Vorobyev, M. (1997). Metric analysis of increment threshold spectral sensitivity in the honeybee. *Vision Research*, 37, 425–439.
- Cole, G. R., Hine, T., & McIlhagga, W. (1993). Detection mechanisms in L-, M-, and S-cone contrast space. *Journal of the Optical Society of America A*, 10, 38–51.
- de Vries, H. L. (1943). The quantum character of light and its bearing upon threshold of vision, the differential sensitivity and visual acuity of the eye. *Physica*, 10, 553–564.
- Dixon, E. R. (1978). Spectral distribution of Australian daylight. *Journal of the Optical Society of America A*, 68, 437–450.
- Dodge, F. A., Jr., Knight, B. W., & Toyoda, J. (1968). Voltage noise in *Limulus* visual cells. *Science*, 160, 88–90.
- Dubs, A., Laughlin, S. B., & Srinivasan, M. V. (1981). Single photon signals and first order interneurons at behavioral threshold. *Journal of Physiology (London)*, 317, 317–334.
- Fain, G. L., Granda, A. M., & Maxwell, J. H. (1977). Voltage signals of photoreceptors at visual threshold. *Nature*, 265, 181–183.
- Giurfa, M., Vorobyev, M., Kevan, P., & Menzel, R. (1996). Detection of coloured stimuli by honeybees: minimum visual angles and receptor specific contrasts. *Journal of Comparative Physiology A*, 178, 699–709.
- Giurfa, M., Vorobyev, M., Brandt, R., Posner, B., & Menzel, R. (1997). Discrimination of coloured stimuli by honeybees: alternative use of achromatic and chromatic signals. *Journal of Comparative Physiology A*, 180, 235–243.
- Giurfa, M., & Vorobyev, M. (1998). The angular range of achromatic target detection by honeybees. *Journal of Comparative Physiology A*, 183, 101–110.
- Goldsmith, T. H. (1991). The evolution of visual pigments and colour vision. In P. Gouras, *The Perception of Colour* (pp. 62–84). London: MacMillan Press.
- Guth, S. L., Massof, R. W., & Benzschawel, T. (1980). Vector model for normal and dichromatic color vision. *Journal of the Optical Society of America A*, 70, 197–211.

- Hecht, S., Shlaer, S., & Pirenne, M. H. (1942). Energy, quanta, and vision. *Journal of General Physiology*, 25, 819–840.
- Helmholtz, H. V. (1896). *Handbuch der physiologischen Optik* (2nd). Hamburg: Voss.
- von Helversen, O. V. (1972). Zur spektralen Unterschiedsempfindlichkeit der Honigbiene. *Journal of Comparative Physiology*, 80, 439–472.
- Hess, R. F., Sharpe, L. T., & Nordby, K. E. (1990). *Night vision*. Cambridge: Cambridge University Press.
- Howard, J., Blakeslee, B., & Laughlin, S. B. (1987). The intracellular pupil mechanism and photoreceptor signal: noise ratios in the fly *Lucilia cuprina*. *Proceedings of Royal Society of London B*, 231, 415–435.
- Jacobs, J. H. (1993). The distribution and nature of colour vision among the mammals. *Biological Review of Cambridge Philosophical Society*, 68, 413–471.
- King-Smith, P. E., & Carden, D. (1976). Luminance and opponent-color contributions to visual detection and adaptation and to temporal and spatial integration. *Journal of the Optical Society of America*, 66, 709–717.
- MacAdam, D. L. (1942). Visual sensitivities to color differences in daylight. *Journal of the Optical Society of America*, 32, 247–255.
- Menzel, R., & Blakers, M. (1976). Colour receptors in the bee eye — morphology and spectral sensitivity. *Journal of Comparative Physiology*, 108, 11–33.
- Menzel, R., & Snyder, A. W. (1975). Introduction to photoreceptor optics — an overview. In A. W. Snyder, & R. Menzel, *Photoreceptor Optics* (pp. 1–13). Berlin–Heidelberg–New York: Springer.
- Menzel, R., & Backhaus, W. (1991). Colour vision in insects. In P. Gouras, *The Perception of colour* (pp. 262–288). London: MacMillan Press.
- Neumeyer, C. (1984). On spectral sensitivity in the goldfish; evidence for neural interactions between different ‘cone mechanisms’. *Vision Research*, 24, 1223–1231.
- Neumeyer, C. (1991). Evolution of colour vision. In J. R. Cronly-Dillon, & R. L. Gregory, *Vision and visual dysfunction. Evolution of the eye and visual system*. London: Macmillan Press Volume 2.
- Peitsch, D., Fietz, A., Hertel, H., de Souza, J., Ventura, D. F., & Menzel, R. (1992). The spectral input systems of hymenopteran insects and their receptor-based colour vision. *Journal of Comparative Physiology A*, 170, 23–40.
- Reichardt, W. (1969). Transduction of single quantum effects. (Evidence from behavioural experiments on the fly). In W. Reichardt, *Processing of optical data by organisms and machines*. New York: Academic Press.
- Rose, A. (1948). The sensitivity performance of the human eye on an absolute scale. *Journal of the Optical Society of America*, 38, 196–208.
- Sankeralli, M. J., & Mullen, K. T. (1996). Estimation of the L-cone, M-cone, and S-cone weights of the postreceptoral detection mechanisms. *Journal of the Optical Society of America A*, 13, 906–915.
- Sperling, H. G., & Harwerth, R. S. (1971). Red-green cone interactions in the increment-threshold spectral sensitivity of primates. *Science*, 172, 180–184.
- Srinivasan, M. V., & Lehrer, M. (1985). Temporal resolution of colour vision in the honeybee. *Journal of Comparative Physiology A*, 157, 579–586.
- Stiles, S. (1946). A modified Helmholtz line element in brightness-colour space. *Proceedings of Physical Society of London*, 58, 41–51.
- Thornton, J. E., & Pugh, E. N. J. (1983). Red/green color opponency at detection threshold. *Science*, 219, 191–193.
- Trabka, A. (1968). On Stiles’ line element in brightness-color space and the color power of the blue. *Vision Research*, 8, 113–134.
- Vorobyev, M., & Brandt, R. (1997). How do insect pollinators discriminate colours? *Israel Journal of Plant Sciences*.
- Vorobyev, M., & Osorio, D. (1998). Receptor noise as a determinant of colour thresholds. *Proceedings of the Royal Society of London B*, 265, 351–358.
- Vorobyev, M., Osorio, D., Bennett, A. T. D., Marshall, N. J., & Cuthill, I. C. (1998). Tetrachromacy, oil droplets and bird plumage colours. *Journal of Comparative Physiology A*, 183, 621–633.
- Warrant, E. J., Porombka, T., & Kirchner, W. (1996). Neural image enhancement allows honeybees to see at night. *Proceedings of the Royal Society of London B*, 261, 1521–1526.
- Wyszecki, G., & Stiles, W. S. (1982). *Color science — concepts and methods, quantitative data and formulae* (2nd). New York: Wiley.
- Yeh, T., Pokorny, J., & Smith, V. C. (1993). Chromatic discrimination with variation in chromaticity and luminance — data and theory. *Vision Research*, 33, 1835–1845.